Probe Diffusion in Aqueous Poly(vinyl alcohol) Solutions Studied by Fluorescence Correlation Spectroscopy

Ariel Michelman-Ribeiro, Ferenc Horkay, Ralph Nossal, and Hacène Boukari*

Laboratory of Integrative and Medical Biophysics, National Institutes of Child Health and Human Development, National Institutes of Health, Bethesda, Maryland 20892

Received December 18, 2006; Revised Manuscript Received March 1, 2007

We report fluorescence correlation spectroscopy measurements of the translational diffusion coefficient of various probe particles in dilute and semidilute aqueous poly(vinyl alcohol) solutions. The range of sizes of the particles (fluorescent molecules, proteins, and polymers) was chosen to explore various length scales of the polymer solutions as defined by the polymer−polymer correlation length. For particles larger than the correlation length, we find that the diffusion coefficient, D, decreases exponentially with the polymer concentration. This can be explained by an exponential increase in the solution viscosity, consistent with the Stokes−Einstein equation. For probes on the order of the correlation length, the decrease of the diffusion coefficient cannot be accounted for by the Stokes−Einstein equation, but can be fit by a stretched exponential, $D \sim \exp(-\alpha c^n)$, where we find $n = 0.73-0.84$ and α is related to the probe size. These results are in accord with a diffusion model of Langevin and Rondelez (*Polymer* **1978**, *19*, 1875), where these values of n indicate a good solvent quality.

Introduction

The past decades have seen extensive use of physics-based techniques (e.g., FCS, FRAP, micro-rheology, micro-DLS) to measure fundamental characteristics of complex biological materials, such as cells in vivo,[1−5] cellular cytoplasm,[6,7] actin and tubulin networks,[8−10] cartilage,[11] and mucin.[12,13] Transport properties of solvent and biomacromolecules in these materials are often vital to their function. However, measurements of transport in these systems are often difficult to interpret, as the solvents and biomacromolecules may interact through electrostatics, hydrodynamics, chemical binding, etc. To gain insight into this problem, it may help to use simpler model systems, composed of synthetic water-soluble polymers, whose properties are better characterized and can be tuned according to particular applications. Here, we use poly(vinyl alcohol) (PVA) as a model system. PVA is a water-soluble, neutral, linear polymer that is an important component of many biotechnological devices, including tissue scaffolds[14−16] and drug delivery devices.[17−19]

Understanding particle diffusion in polymer solutions remains problematic despite extensive theoretical and experimental efforts. In pure solvents, the basis for modeling the diffusion of non-interacting particles is represented by the Stokes−Einstein relation, $D = k_B T/6\pi\eta R_H$, where D is the diffusion coefficient, k_B is the Boltzmann constant, T is the temperature, η is the solvent viscosity, and R_H is the hydrodynamic radius. One notable assumption in the derivation of the Stokes−Einstein equation is the treatment of the host solvent as a continuum,[20] at least on the length scale of the size of the particle, R. In the case of particle diffusion in polymer solutions, however, the system should be considered as ternary, consisting of solvent, polymer, and probe, and the characteristics of all of these components must be taken into account.[21]

The thermodynamic behavior of an ideal polymer solution in the semidilute concentration regime is governed by the polymer−polymer correlation length, ξ, introducing a second length scale in addition to the probe size R. For probe diffusion, three regimes can be identified, depending on the relative size R/ξ, as shown in Figure 1. For $R/\xi \gg 1$ (Figure 1c), probe diffusion can often be described by the Stokes−Einstein expression, which depends mainly on the viscosity of the host polymer/solvent solution. For $R/\xi \ll 1$ (Figure 1a), the probe may be so small that it detects the pure solvent viscosity. For $R/\xi \sim 1$ (Figure 1b), the particle should see a rather inhomogeneous local environment at length scale ξ, and its diffusive behavior is not necessarily governed by the bulk viscosity of solvent/polymer solution. In this regime, a general consensus on what physical parameters should be included in a model has yet to be reached.[22−25]

Techniques traditionally used to study probe diffusion in polymer solutions include centrifugation (sedimentation),[26,27] pulsed field-gradient nuclear magnetic resonance (PFG NMR),[28] and dynamic light scattering (DLS).[29−33] Centrifugation is a relatively invasive technique, as large forces are applied to the sample; it is also somewhat restricted in application, because the polymer and solvent should have similar densities. PFG NMR has limitations related to spin−spin relaxation times, the magnetic gradient strength, and eddy currents. In DLS, both the probes and the polymers contribute to the scattering signal, making it difficult to resolve the motion of the probe from that of the background polymers. For this reason, larger probes have been used (>20 nm), which in most situations would preclude exploration of the regime $R/\xi \sim 1$.

Recently, techniques such as fluorescence recovery after photobleaching (FRAP)[20,21,34] and fluorescence correlation spectroscopy (FCS)[35−37] have been shown to be powerful tools to measure diffusion of fluorescent particles in complex media. In FRAP, an intense laser beam illuminates a small volume of the sample, in principle causing irreversible photobleaching of the fluorescent particles. As particles from outside the photobleached region diffuse in, the intensity of their fluorescence is detected over time, and their translational diffusion can be obtained. However, FRAP must be applied carefully as analysis of the data is complicated by several factors.[20,38] In the ideal

* Corresponding author. E-mail: boukarih@mail.nih.gov.

10.1021/bm061195r
Published on Web 04/19/2007

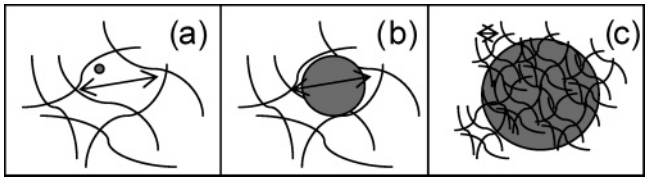

Figure 1. Schematic diagram depicting three regimes of relative sizes of probes and the correlation lengths (indicated by arrow) of the polymer solutions in which they are diffusing. In (a) the probe is much smaller than the correlation length, in (b) the probe is on the order of the correlation length, and in (c) the probe is much larger than the correlation length. FCS can be applied to study these three regimes.

case, the sample is completely photobleached, and the subsequent increase in fluorescence is due solely to diffusion of a single fluorescent species, until the initial pre-bleach level of fluorescence is recovered. This ideal situation can be compromised if there are immobile fluorescent particles or very slow diffusion of some particles. Also, the photobleaching is sometimes reversed, which can confound the interpretation of the data.

FCS is an optical technique in which the time correlation of fluctuations in detected fluorescence intensity can be used to determine details of the dynamics of the particles (such as the diffusion coefficient). In FCS, a laser excites fluorescence of particles in a sample, and the fluorescence intensity is measured from a very small volume (~1 fL). As the particles diffuse in and out of the volume, the fluorescent signal fluctuates, and the time-correlation of the signal can be analyzed to reveal the particle dynamics. One of the advantages of FCS is that it can reveal, in principle, not only diffusion information, but also the average number of detected particles. This can be useful for studying systems in which the particle is involved in binding reactions[39] or to ensure there is no sedimentation or photobleaching of particles. FCS is a minimally invasive technique because a very low concentration of fluorescent particles (nanomolar) is added to the sample and the laser flux is low (below the threshold for photobleaching). Another advantage to using a technique that detects labeled particles is that different types of particles can be given different labels, allowing different populations to be distinguished and the dynamics of their interactions to be studied. FCS can also be used with a wide range of particle sizes, from ~1 nm (such as single molecules) to >100 nm (such as polymers, proteins, or nanospheres). For these reasons, FCS is an ideal choice for studying diffusion in complex systems and exploring various length scales, as shown in Figure 1.

We used FCS to measure the translational diffusion coefficients of various fluorescent particles (TAMRA, Rhodamine 6G, Alexa546, (*R*)-phycoerythrin; rhodamine-labeled dextran, bovine serum albumin, polystyrene beads) in PVA solutions in the dilute and semidilute regimes. These particles span a range of sizes that allow us to explore the two regimes shown in Figure 1b and c. We have determined the apparent diffusion coefficients of these particles as a function of the polymer concentration at room temperature. Here, we apply a model of diffusion developed in the polymer physics community to elicit an understanding of the behavior of fluorescent probes in a model biological system. Using a variety of fluorescent probes, we search for a universal behavior of probe diffusion, independent of specific interactions due to the chemistry of the probes, polymer, and solvent. In this paper, we first introduce some models of probe diffusion, presenting the equations to be tested by the data. Next, we show data for large particles and then small particles diffusing in PVA solutions and discuss the results in the context of the models. Finally, we provide a physical interpretation of the model parameters.

Materials and Methods

Sample Preparation. All chosen fluorescent probes are water-soluble and were purchased from Invitrogen (Molecular Probes). These include the following molecular bright fluorescent dyes: 5-carboxytetramethylrhodamine (TAMRA) (M_w = 430 Da, Abs:Em 555:580 nm), Alexa546 (M_w = 1070 Da, Abs:Em 556:575 nm), and 6-carboxyrhodamine 6G (R6G) (M_w = 556 Da, Abs:Em 525:555 nm). We also used the naturally fluorescent phycobiliprotein, (*R*)-phycoerythrin (M_w = 240 000, Abs:Em 546:578 nm), which is derived from cyanobacteria and eukaryotic algae. The other probes were exogenously labeled particles: TAMRA-labeled dextran (M_w = 10 000 Da), TAMRA-labeled bovine serum albumin (BSA) (M_w = 66 000 Da), and rhodamine-labeled polystyrene latex spheres (44 nm diameter, Abs:Em 540:560 nm). While dextran is a branched sucrose polymer, BSA, (*R*)-phycoerythrin, and polystyrene are globular particles.

PVA (Sigma Aldrich, M_w = 85 000 Da, degree of hydrolysis >99%) was dissolved in deionized water at 95 °C. The entanglement concentration is between 2 and 3% w/v. Solutions were diluted from a stock solution to concentrations ranging from 1 to 8.6% w/v. The correlation length of identical solutions has been characterized by SANS measurements and varies from approximately 12 to 2 nm across this concentration range.[40,41] Solutions were heated at 85 °C for several hours prior to experimentation to minimize hydrogen bonding between PVA chains. Once the solutions cooled to room temperature, nanomolar concentrations of fluorescent particles were added. The samples sat for approximately 15 h to ensure that the particles had time to diffuse uniformly and then were loaded into small (~65 μL) sample chambers (secure seal hybridization chambers, Grace Bio-Labs) on glass coverslips for FCS measurements.

FCS Setup. Two FCS instruments were used in these experiments: a custom-built FCS instrument[39] with a 543 nm excitation line from a HeNe laser, and a commercial instrument from Hamamatsu (model C9413), with a 473 nm excitation wavelength from a solid-state laser.

In the custom-built instrument, the beam was first expanded and then focused onto the sample to a diameter of approximately 1 μm with a 60X, 1.2 N.A. water immersion objective, which was also used to collect the emitted fluorescent light. This emitted beam was split with a 50/50 cube prism into two beams that were focused by additional lenses onto two optical fibers connected to separate avalanche photodiode detectors (APD), creating a pinhole-like confocal detection setup. The signals from the two APDs were time cross-correlated, which reduces possible after-pulsing effects that can be important at short times (<10 μs). A digital correlator board (Brookhaven Instrument) processed the signals and calculated correlation functions. The incident laser light was attenuated to reduce photobleaching and to avoid photosaturation effects.[42] For TAMRA and TAMRA-labeled particles, reduction to 27 μW was sufficient, but for (*R*)-phycoerythrin, the power was reduced to 0.3 μW. These values were found through a systematic study of intensity effects on the correlation functions.

The newly marketed Hamamatsu instrument is a compact, portable device. It is equipped with a 473 nm LD-pumped solid-state laser, a high sensitivity photomultiplier tube with low afterpulsing, a 25 μm diameter pinhole confocal detection, a water-immersion objective (Olympus UApo 40X W/340; N.A. = 1.15), and built-in correlator board. In most measurements, the 1 mW input laser beam was attenuated to 10 μW, and the emission filter cutoff wavelength was set to 495 nm. The instrument comes with a software package that can be readily used to fit the measured correlation functions.

FCS Measurements. FCS measures the intensity correlation function,[43,44]

$$F(\tau) = 1 + \frac{\langle \delta I(t) \delta I(t+\tau) \rangle}{\langle I(t) \rangle^2} \qquad (1)$$

Table 1. Effective Hydrodynamic Diameters of the Various Probe Particles and the Values of the Exponent and Prefactor Determined from Eq 8

probe	d_h (nm)	n	α
Rhodamine6G	1.6	0.77	0.23
TAMRA	1.6	0.73	0.28
Alexa546	1.9	0.84	0.23
dextran	4.4	0.78	0.27
BSA	9.4	0.82	0.41
(*R*)-phycoerythrin	11.8	0.84	0.48

where $\delta I(t) = I(t) - \langle I(t)\rangle$ denotes the deviation of the intensity $I(t)$ emitted by the fluorescent particles at time t from the average intensity, $\langle I(t)\rangle$. For monodisperse particles diffusing freely in a solution, eq 1 can be written as:[39,44]

$$F(\tau) = 1 + \frac{1}{N}\frac{1}{\left(1+\frac{\tau}{\tau_d}\right)}\frac{1}{\left(1+p\frac{\tau}{\tau_d}\right)^{1/2}} \quad (2)$$

Here, r_0 and z_0 characterize the ideal Gaussian profile ($W(r,z) = Ae^{-2(r/r_0)^2}e^{-2(z/z_0)^2}$) of the focused excitation beam, N denotes the average number of particles in the excitation volume, $p = (r_0/z_0)^2$ is a constant, and $\tau_d = r_0^2/4D$ is the diffusion time, where D is the translational diffusion coefficient.

If there are two independent diffusing species, the correlation function correspondingly becomes:[45]

$$F(\tau) = 1 + m_1\frac{1}{\left(1+\frac{\tau}{\tau_1}\right)}\frac{1}{\left(1+p\frac{\tau}{\tau_1}\right)^{1/2}} + m_2\frac{1}{\left(1+\frac{\tau}{\tau_2}\right)}\frac{1}{\left(1+p\frac{\tau}{\tau_2}\right)^{1/2}} \quad (3)$$

where m_1 and m_2 are related to the quantum yield and average numbers of each of the diffusing species in the sampling volume, and τ_1 and τ_2 are the diffusion times of the two species. Often with a fluorescently labeled probe it is difficult to extract all of the free dye from the solution, making it necessary to use eq 3, where one diffusing species is the free dye and the other is the labeled probe.

Several FCS measurements were made on each sample. Measurements made at different locations within a sample yielded identical results, indicating the samples were homogeneous on the length scale of the illuminated volume. All of the experiments were performed at approximately 22 °C.

Viscosity Measurements. The viscosity of the lower concentration PVA solutions (<3% w/v) was measured using a falling ball in a capillary tube (Automatic MicroViscometer). The viscosity of the higher concentration solutions (>3% w/v) was measured using a cone-plate rheometer (Advanced Rheometer AR2000).

Probe Size Characterization. We used R6G ($D = 2.8 \times 10^{-6}$ cm^2/s)[46] to calibrate both FCS instruments. The hydrodynamic diameter of the probes can be determined from FCS measurements of the diffusion of the probes in water, using the Stokes−Einstein relation. These values are listed in Table 1 (except for polystyrene). The sizes of the dextran, BSA, (*R*)-phycoerythrin, and polystyrene are consistent with those derived from DLS measurements.[47,48] We will compare the probe sizes with the correlation length in our PVA solutions, which is approximately 4 nm at 4% w/v, and varies from around 12 to 2 nm across the concentration range studied here.[40,41]

Probe Diffusion Models

It is still not completely agreed upon what aspects of the ternary system (probe/solvent/polymer) affect probe diffusion when the probes are on the order of the correlation length.[20,22,29] Many models have been put forth considering such factors as obstruction effects, hydrodynamics, and free volume theory.[22] One of the challenges in testing proposed models in this regime is a paucity of data; most experiments have been performed in the region $R \gg \xi$.[30,32,33,49,50]

One of the favored models was developed by de Gennes, Langevin, and Rondelez.[26] Generally, de Gennes argues for the influence of topological effects on probe behavior.[51] In this model, the semidilute polymer solution is treated as a transient statistical network of mesh size ξ. The frictional force on the particle should be different if R is less than or greater than ξ. A scaling law has been suggested by de Gennes, Pincus, and Velasco in a communication with Langevin and Rondelez:[26]

$$\frac{f_0}{f_c} = \Psi\left(\frac{R}{\xi}\right) \quad (4)$$

where f_0 and f_c are the friction coefficients of a probe moving in pure solvent and in a solution of polymer concentration c, respectively. In the regime $R/\xi \sim 1$, Langevin and Rondelez (based on a communication with de Gennes) have suggested a specific function for $\Psi(R/\xi)$ for the analysis of their sedimentation data:[26]

$$\Psi\left(\frac{R}{\xi}\right) = e^{-(R/\xi)^\delta} \quad (5)$$

where δ is a scaling parameter. Equation 5 was obtained by estimating the reduction of entropy due to distortion of the mesh unit of size ξ by the particle of size R. This model is attractive because it is relatively simple and takes into account two seemingly obvious parameters: R and ξ. Experimentally, Langevin and Rondelez found the value $\delta = 1$ for sedimentation of Ludox, bovine serum albumin (BSA), and viruses in poly(ethylene oxide) solutions, in agreement with predictions of several models of probe diffusion.[52−54]

From the Nernst−Einstein equation, one has $f_0/f_c = D/D_0$, so eq 5 can be rewritten (with $\delta = 1$) as:

$$\frac{D}{D_0} \sim e^{-(R/r)(c/c^*)^n} \quad (6)$$

where we have utilized de Gennes's scaling relation for ξ, the correlation length in a semidilute solution,[57]

$$\xi \sim r\left(\frac{c}{c^*}\right)^{-n} \quad (7)$$

Here, r is the average polymer chain size, c^* is the concentration where the chains begin to entangle, and n is a scaling parameter related to the polymer chain excluded volume, which reflects the solvent quality. For a theta solvent, $n = 1$, and for a good solvent, $n = {}^3/_4$.[57] Note that eq 6 can be rewritten as:

$$\frac{D}{D_0} \sim e^{-\alpha c^n} \quad (8)$$

where

$$\alpha \sim \frac{R}{r}c^{*-n} \quad (9)$$

Another model of probe diffusion has been developed by Phillies, who argues that probe diffusion is largely governed by hydrodynamic interactions, as opposed to topological effects such as entanglements.[49,50,55,56] Phillies asserts that this physical

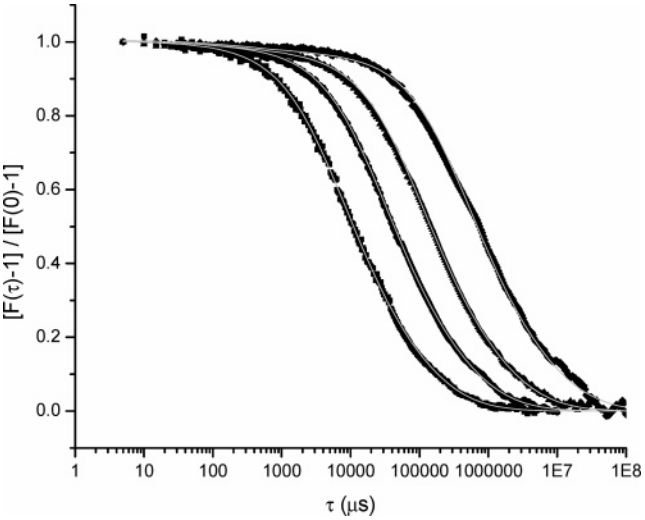

Figure 2. Normalized FCS correlation functions for 44 nm polystyrene latex spheres in PVA solutions of various concentrations (left to right curves are for 1, 3.2, 5, and 8% w/v PVA). Solid lines are fits of the data with the normalized expression of eq 3.

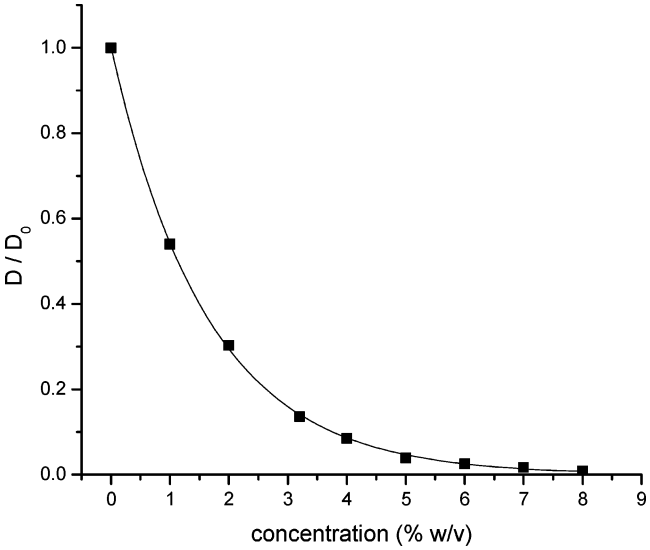

Figure 3. Scaled diffusion coefficients of 44 nm polystyrene latex spheres as a function of PVA concentration. D_0 is the diffusion coefficient of the sphere in water. D and D_0 were obtained from fits to FCS correlation data using eq 2. The decrease in diffusion coefficient is well described by a pure exponential (see solid line).

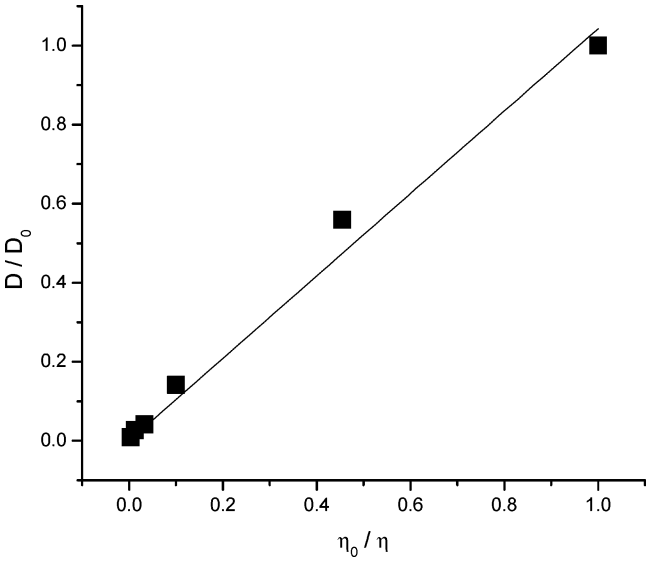

Figure 4. Scaled diffusion coefficients of 44 nm polystyrene latex spheres in PVA solutions (measured by FCS) as a function of scaled viscosity of these solutions (measured by bulk rheological techniques). The data are fit to a line through the origin with a slope of 1, consistent with the Stokes−Einstein equation, indicating that the 44 nm probes measure changes in the bulk viscosity.

assumption differs from the assumptions made in the de Gennes[57] and Doi−Edwards[58] models, where topological constraints dominate hydrodynamic forces.[56] His expression for probe diffusion in polymer solutions, however, has the same form as eq 8, where α and n are adjustable parameters.[50] He finds that α has a dependence on the polymer molecular weight but not probe size, and n is related to solvent quality.[50]

Although theoretical treatments by Langevin and Rondelez,[26] Phillies,[49,50,55,56] Cukier,[52] Altenberger,[53] and Amsden[25] are based on different physical mechanisms, they all develop formulas for the scaled diffusion of probes, which can be expressed in the form of a stretched exponential function of the polymer concentration. This equation has been found to fit a wide variety of experimental data,[22,26,29,32,51] with values of n reported between 0.5 and 1.[22] We apply eq 8 to our data, and test whether the prefactor α depends on probe size, as in eq 9, and whether n can be interpreted as related to the solvent quality.

Results and Discussion

Diffusion of Large Probes in PVA Solutions ($R \gg \xi$). Normalized correlation functions of the polystyrene latex spheres in solutions of various concentrations of PVA are shown in Figure 2. The correlation functions are shifted to longer diffusion times as the polymer concentration increases. As there was a small amount of free dye in the sample, we fit the correlation functions with eq 3, allowing values of τ to be determined for each solution. For purposes of comparison, it is convenient to divide the characteristic time, τ_d, by the diffusion time of the probe in water, τ_d(water), to yield a scaled quantity. The inverse of the scaled diffusion time is equal to the scaled diffusion coefficient, D/D_0, which is plotted as a function of the PVA concentration in Figure 3. Note that the scaled diffusion coefficient can be readily fit with a single exponential ($D/D_0 = \exp(-bc)$, with $b = 0.61$). Because $R \gg \xi$, we would expect the Stokes−Einstein equation to describe the diffusion of the polystyrene particles in these PVA solutions. That is, $D/D_0 = \eta_0/\eta$, where D and D_0 are the diffusion coefficients of the probes in the polymer solution and solvent, respectively, and η and η_0 are the viscosities of the solution and solvent, respectively. Indeed, when D/D_0 is plotted as a function of η_0/η (see Figure 4), it is seen that the data are well fit to a line through the origin and the decrease of the diffusion coefficient of the polystyrene spheres can be linked to the increase in the bulk viscosity of the polymer solution.

Diffusion of Small Probes in PVA Solutions ($R \sim \xi$). The smallest probes studied were TAMRA, R6G, Alexa546, and dextran, which are all in the range $R \sim \xi$. BSA and (*R*)-phycoerythrin are slightly larger than the correlation length over most of the concentrations here. Representative data (obtained from dextran probes) of normalized correlation functions at several concentrations of PVA solutions are shown in Figure 5.

The curves are shifted to longer diffusion times as the PVA concentration increases. The solid curves are fits to the data of eq 2, which yield a single characteristic diffusion time for the dextran in PVA solutions. We obtained similar curves for R6G,

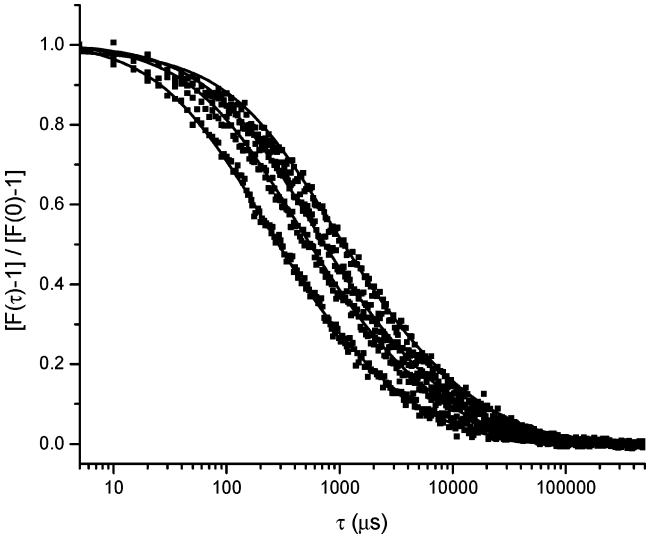

Figure 5. Normalized correlation functions for dextran in PVA solutions of various concentrations (left to right curves are for 0, 3.2, 5, and 8% w/v PVA). The solid curves are fits of the data with the normalized expression of eq 2.

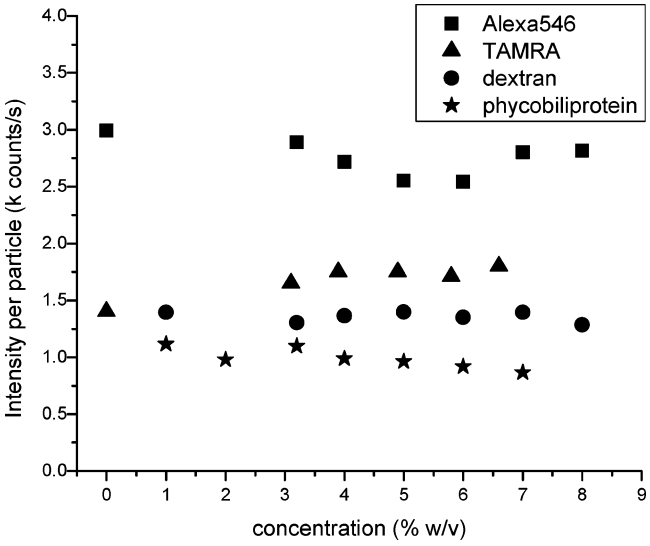

Figure 6. Average intensity per particle as a function of PVA concentration for Alexa546, TAMRA, dextran, and (*R*)-phycoerythrin. The curves are relatively flat across this concentration range, suggesting that the particles do not become immobilized.

TAMRA, Alexa546, and (*R*)-phycoerythrin diffusing in PVA solutions. From the fits of eq 2, we extract N and τ_d. Because N is a measure of the average number of diffusing particles, it is important to examine this quantity because it may indicate immobilization, photobleaching, or sedimentation. When the detected intensity is divided by N, an average intensity per particle is obtained. Figure 6 shows the average intensity per particle in PVA samples of various concentrations for several different probes. The intensity per particle is approximately constant, regardless of PVA concentration. This suggests that the presence of PVA does not significantly enhance or diminish fluorescence of these molecules and, more importantly, that the particles do not become immobilized as the solution becomes more concentrated.

For the BSA samples, we found that there was a small amount of free TAMRA in the labeled-BSA solution and that the correlation functions consequently were not well fit by eq 2. We therefore fit the correlation functions with eq 3, for two diffusing species, and fixed the diffusion time of one of the

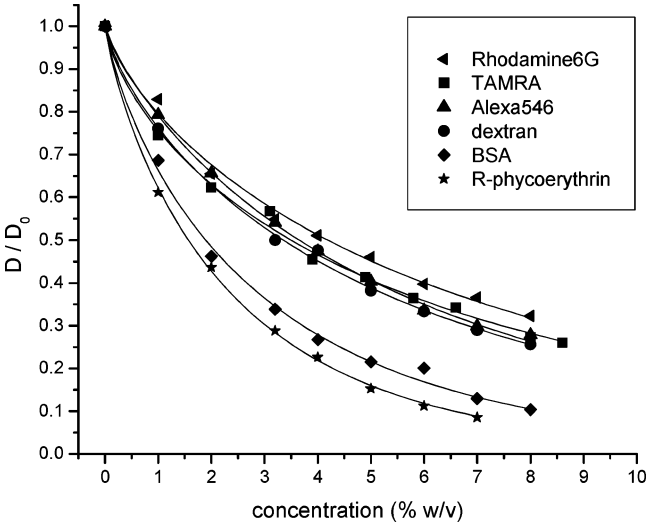

Figure 7. Scaled diffusion coefficients of various probes as a function of PVA concentration. The solid lines are fits of the data with the stretched exponential (eq 8), α and n being the fitting parameters. Values of the parameters are given in Table 1.

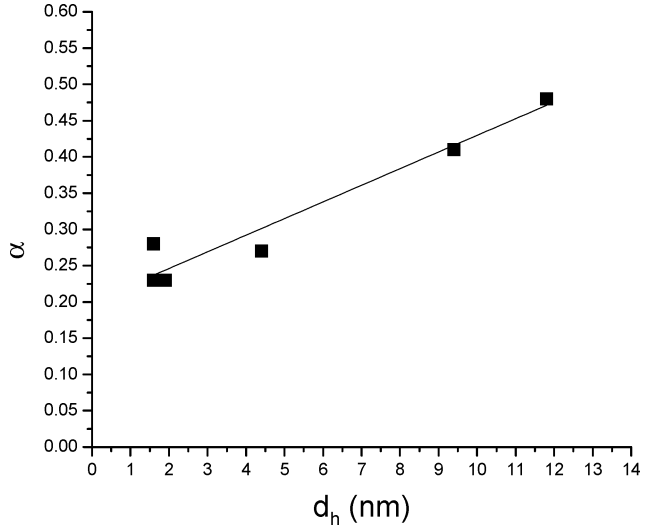

Figure 8. The parameter α from eq 8 shows a linear dependence on the probe diameter.

species to that of TAMRA in the corresponding PVA solution. Again, we divide the characteristic time, τ_d, by τ_d(water) (the diffusion time of the particular probe in water), and convert this scaled diffusion time to D/D_0. Figure 7 shows the scaled diffusion coefficients as a function of polymer concentration for the Rhodamine6G, TAMRA, Alexa546, dextran, BSA, and (*R*)-phycoerythrin probes. Unlike the polystyrene data, the diffusion coefficients of these small probes cannot be fit with a simple exponential, and thus the decay of the diffusion coefficient here cannot be attributed to the increase in solution viscosity. Instead, the data are well fit by a stretched exponential ($D/D_0 = \exp(-\alpha c^n)$), and values of the free parameters α and n are as given in Table 1. These probes, which are in the region $R \sim \xi$, all exhibit a similar exponent, n close to 0.75, corresponding to a good solvent. This is consistent with results from osmotic pressure measurements on a similar aqueous PVA system.[40] It is interesting to note that the scaled diffusion coefficients of the smallest probes fall on almost the same curve, while those of the slightly larger probes fall on different curves. This suggests that the probes may experience different local dynamics, although they seem to detect the same solvent quality because they all yield similar values of n.

Figure 8 shows a plot of the fitting parameter α as a function of particle size, suggesting a linear dependence. This is consistent with the model of Langevin and Rondelez, where the scaled diffusion coefficient depends on the probe size (eq 9). Note that it is not necessary for the *y*-intercept to be 0 because as R approaches 0, the system enters a regime where eq 9 is not valid (eq 9 applies where $R/\xi \sim 1$).

Conclusions

FCS is a reliable technique for measuring the diffusion coefficients of fluorescent probes in dilute and semidilute polymer solutions.[59,60] We have studied a variety of sizes of probes in the context of the Langevin−Rondelez and Phillies models and have discussed the physical meaning of the fitting parameters. The 44 nm polystyrene latex particles were large enough, as compared to the correlation length of the PVA solutions, that they can be considered in the regime $R \gg \xi$. The diffusion coefficient decayed exponentially with polymer concentration, and this behavior can be attributed to the exponential increase of the bulk viscosity of the polymer solution with the polymer concentration. When the measured diffusion coefficient is used to calculate the viscosity through the Stokes−Einstein equation, those viscosity values were found to be reasonably close to the experimentally measured bulk viscosity. This suggests a novel use of FCS to monitor the bulk viscosity of polymer solutions.

The diffusion coefficients of the probes in the regime $R \sim \xi$ (R6G, TAMRA, Alexa546, dextran, BSA, and (*R*)-phycoerythrin) all followed the theoretical prediction of a stretched exponential as a function of concentration. In the models of both Phillies and Langevin and Rondelez, the exponent n is expected to be related to the solvent quality. For these small probes, values of n in the range 0.73−0.84 were obtained. This suggests that water is a good solvent for PVA, which is consistent with our interpretation of the DLS data taken in the dilute regime of the PVA solution. One of the distinguishing aspects between the two models is that Phillies does not predict a dependence on the particle size, while Langevin and Rondelez predict a linear dependence of the prefactor α on R. Indeed, we found that α scales linearly with the particle size.

Acknowledgment. We would like to thank Dan Sackett for insightful discussions, Rodolfo Ghirlando for use of his light-scattering instrument, Hamamatsu for use of their FCS instrument, and Priya Patel for her help with the data. This work was supported by intramural funds from the National Institute of Child Health and Human Development, NIH. A.M-R. is the recipient of a predoctoral Intramural Research Training Award from the National Institute of Child Health and Human Development.

References and Notes

(1) Daniels, B. R.; Masi, B. C.; Wirtz, D. *Biophys. J.* **2006**, *90*, 4712.
(2) Dauty, E.; Verkman, A. S. *J. Biol. Chem.* **2005**, *280*, 7823.
(3) Vukojevic, V.; Pramanik, A.; Yakovleva, T.; Rigler, R.; Terenius, L.; Bakalikin, G. *Cell. Mol. Life Sci.* **2005**, *62*, 535.
(4) Yamada, S.; Wirtz, D.; Kuo, S. C. *Biophys. J.* **2000**, *78*, 1736.
(5) Berland, K. M.; So, P. T. C.; Gratton, E. *Biophys. J.* **1995**, *68*, 694.
(6) Arrio-Dupont, M.; Foucault, G.; Vacher, M.; Devaux, P. F.; Cribier, S. *Biophys. J.* **2000**, *78*, 901.
(7) Seksek, O.; Biwersi, J.; Verkman, A. S. *J. Cell Biol.* **1997**, *138*, 131.
(8) McGrath, J. L. *Curr. Biol.* **2006**, *16*, R800.
(9) Valentine, M. T.; Perlman, Z. E.; Gardel, M. L.; Shin, J. H.; Matsudaira, P.; Mitchison, T. J.; Weitz, D. A. *Biophys. J.* **2004**, *86*, 4004.
(10) McGrath, J. L.; Hartwig, J. H.; Tardy, Y.; Dewey, C. F. *Microsc. Res. Tech.* **1998**, *43*, 385.
(11) Papagiannopoulos, A.; Waigh, T. A.; Hardingham, T.; Heinrich, M. *Biomacromolecules* **2006**, *7*, 2162.
(12) Afdhal, N. H.; Cao, X. X.; Bansil, R.; Hong, Z. N.; Thompson, C.; Brown, B.; Wolf, D. *Biomacromolecules* **2004**, *5*, 269.
(13) Celli, J.; Gregor, B.; Turner, B.; Afdhal, N. H.; Bansil, R.; Erramilli, S. *Biomacromolecules* **2005**, *6*, 1329.
(14) Degirmenbasi, N.; Kalyon, D. M.; Birinci, E. *Colloids Surf., B* **2006**, *48*, 42.
(15) Lee, K. Y. *Macromol. Res.* **2005**, *13*, 277.
(16) Cascone, M. G.; Lazzeri, L.; Sparvoli, E.; Scatena, M.; Serino, L. P.; Danti, S. *J. Mater. Sci.: Mater. Med.* **2004**, *15*, 1309.
(17) Peppas, N. A.; Kim, B. *J. Drug Delivery Sci. Technol.* **2006**, *16*, 11.
(18) Wittmar, M.; Unger, F.; Kissel, T. *Macromolecules* **2006**, *39*, 1417.
(19) Agnihotri, S. A.; Aminabhavi, T. M. *Drug Dev. Ind. Pharm.* **2005**, *31*, 491.
(20) Cheng, Y.; Prud'homme, R. K.; Thomas, J. L. *Macromolecules* **2002**, *35*, 8111.
(21) Bu, Z.; Russo, P. S. *Macromolecules* **1994**, *27*, 1187.
(22) Masaro, L.; Zhu, X. X. *Prog. Polym. Sci.* **1999**, *24*, 731.
(23) Kwak, S.; Lafleur, M. *Macromolecules* **2003**, *36*, 3189.
(24) Davies, I. A.; Griffiths, P. C. *Macromolecules* **2003**, *36*, 950.
(25) Amsden, B. *Polymer* **2002**, *43*, 1623.
(26) Langevin, D.; Rondelez, F. *Polymer* **1978**, *19*, 1875.
(27) Tong, P.; Ye, X.; Ackerson, B. J.; Fetters, L. J. *Phys. Rev. Lett.* **1997**, *79*, 2363.
(28) Masaro, L.; Zhu, X. X. *Can. J. Anal. Sci. Spectrosc.* **1998**, *43*, 81.
(29) van der Gucht, J.; Besseling, N. A. M.; Knoben, W.; Bouteiller, L.; Cohen Stuart, M. A. *Phys. Rev. E* **2003**, *67*, 051106.
(30) Won, J.; Onyenemezu, C.; Miller, W. G.; Lodge, T. P. *Macromolecules* **1994**, *27*, 7389.
(31) Nishio, I.; Reina, J. C.; Bansil, R. *Phys. Rev. Lett.* **1987**, *59*, 684.
(32) Reina, J. C.; Bansil, R.; Konak, C. *Polymer* **1990**, *31*, 1038.
(33) Shibayama, M.; Isaka, Y.; Shiwa, Y. *Macromolecules* **1999**, *32*, 7086.
(34) Busch, N. A.; Kim, T.; Bloomfield, V. A. *Macromolecules* **2000**, *38*, 5932.
(35) Michelman-Ribeiro, A.; Boukari, H.; Nossal, R.; Horkay, F. *Macromolecules* **2004**, *37*, 10212.
(36) Liu, R.; Gao, X.; Adams, J.; Oppermann, W. *Macromolecules* **2005**, ma0511090.
(37) Kang, K.; Gapinski, J.; Lettinga, M. P.; Buitenhuis, J.; Meier, G.; Ratajczyk, M.; Dhont, J. K. G.; Patkowski, A. *J. Chem. Phys.* **2005**, *122*, 044905.
(38) Verkman, A. S. *Trends Biochem. Sci.* **2002**, *27*, 27.
(39) Boukari, H.; Nossal, R.; Sackett, D. L. *Biochemistry* **2003**, *42*, 1292.
(40) Geissler, E.; Horkay, F.; Hecht, A. M. *Macromolecules* **1991**, *24*, 6006.
(41) Horkay, F.; Hecht, A.-M.; Geissler, E. *Macromolecules* **1994**, *27*, 1795.
(42) Nagy, A.; Wu, J. R.; Berland, K. M. *J. Biomed. Opt.* **2005**, *10*, Art. No. 044015.
(43) Webb, W. W. *Appl. Opt.* **2001**, *40*, 3969.
(44) Aragon, S. R.; Pecora, R. *J. Chem. Phys.* **1976**, *64*, 1791.
(45) Krichevsky, O.; Bonnet, G. *Rep. Prog. Phys.* **2002**, *65*, 251.
(46) Fatin-Rouge, N.; Starchev, K.; Buffle, J. *Biophys. J.* **2004**, *86*, 2710.
(47) Pharmacosmos, www.dextran.net/dextran_physicalproperties.html.
(48) Bulone, D.; Martorana, V.; San Biagio, P. L. *Biophys. Chem.* **2001**, *91*, 61.
(49) Phillies, G. D. J.; Brown, W.; Zhou, P. *Macromolecules* **1992**, *25*, 4948.
(50) Phillies, G. D. J.; Clomenil, D. *Macromolecules* **1993**, *26*, 167.
(51) de Gennes, P.-G. *Macromolecules* **1976**, *9*, 594.
(52) Cukier, R. I. *Macromolecules* **1984**, *17*, 252.
(53) Altenberger, A. R.; Tirrell, M. *J. Chem. Phys.* **1984**, *80*, 2208.
(54) Ogston, A. G.; Preston, B. N.; Wells, J. D. *Proc. R. Soc. London, Ser. A* **1973**, *333*, 297.
(55) Phillies, G. D. J. *Macromolecules* **1987**, *20*, 558.
(56) Phillies, G. D. J. *J. Non-Cryst. Solids* **1991**, *131*−*133*, 612.
(57) De Gennes, P.-G. *Scaling Concepts in Polymer Physics*; Cornell University Press: Ithaca, NY, 1979.
(58) Doi, M.; Edwards, S. F. *The Theory of Polymer Dynamics*; Clarendon: Oxford, U.K., 1986.
(59) Szymanski, J.; Patkowski, A.; Wilk, A.; Garstecki, P.; Holyst, R. *J. Phys. Chem. B* **2006**, *110*, 25593.
(60) Kang, K.; Wilk, A.; Buitenhuis, J.; Patkowski, A.; Dhont, J. K. G. *J. Chem. Phys.* **2006**, *124*, 044907.

BM061195R